Electronic Supplementary Material (ESI) for Nanoscale Horizons.

Supplemental Materials

InP/ZnS quantum dot photoluminescence modulation *via in situ* H_2S interface engineering

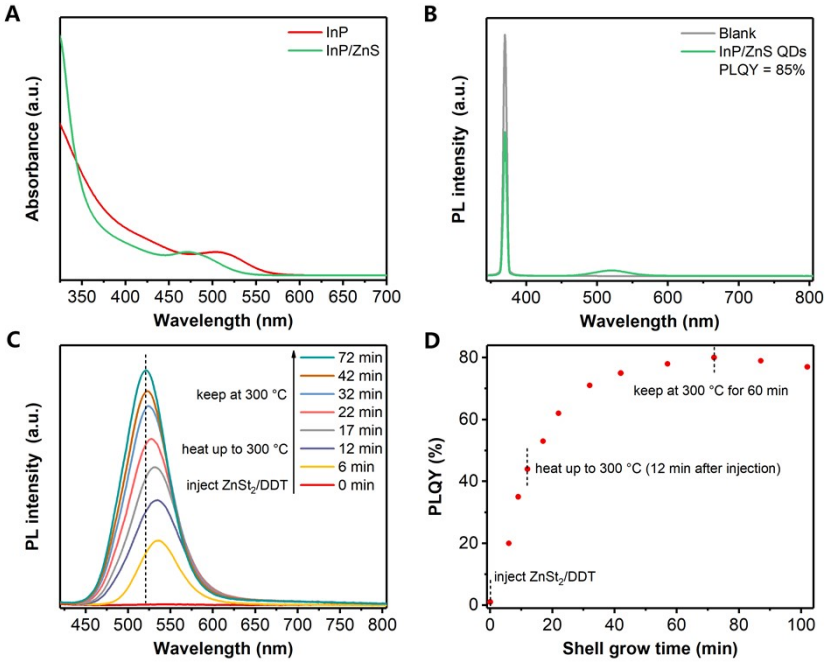

Figure S1. (A) Absorption spectra of InP and InP/ZnS QDs with an enlarger coordinate axis. (B) Absolute PLQY measurement of InP/ZnS QDs. (C) PL spectra and (D) the corresponding PLQY change of InP/ZnS QDs synthesized during different shell formation times. For the heating mantle used in our system, about 12 min are needed for the reaction solution to raise to 300 °C.

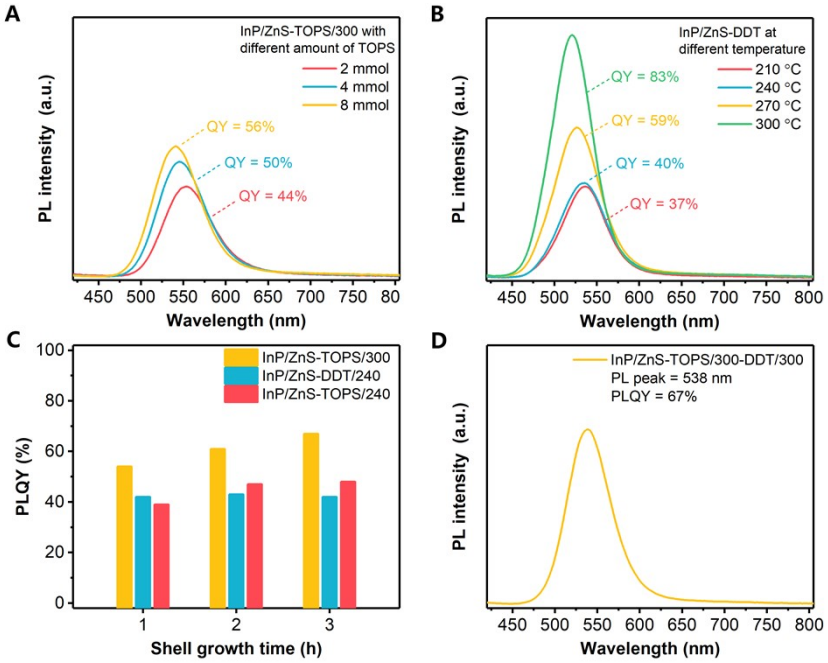

Figure S2. (A) PL spectra of InP/ZnS QDs synthesized with $ZnSt_2$ and different amounts of TOPS at 300 °C during the shell growth. (B) PL spectra of InP/ZnS QDs synthesized with $ZnSt_2$ and DDT at different temperatures during the shell growth. (C) PLQY results of InP/ZnS QDs synthesized with $ZnSt_2$ and TOPS at 300 °C or DDT at 240°C by different reaction times. (D) PL spectrum for InP/ZnS QDs synthesized with a mixture of TOPS and DDT. Briefly, after the core formation, $ZnSt_2$ and 4 mmol TOPS was first added and kept heating at 300 °C for 30 min, then 4 mmol DDT were slowly injected in 5 min and kept at 300 °C for another 30 min.

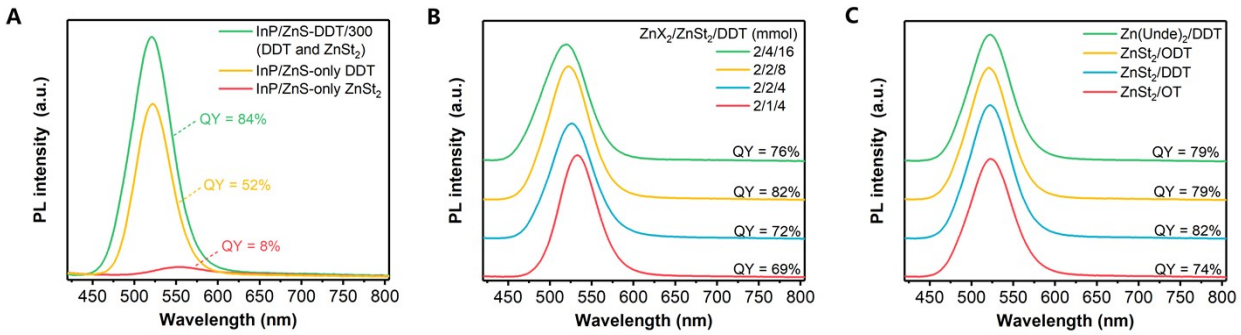

Figure S3. (A) PL spectra of InP/ZnS QDs synthesized with the single precursor of $ZnSt_2$ or DDT at 300 °C during the shell growth. Note that 2 mmol ZnX_2 (1.5 mmol $ZnCl_2$ and 0.5 mmol ZnI_2) were introduced at the beginning of InP core formation. Therefore, there was still Zn resource for ZnS shell formation with DDT during the shell growth process. (B) The photoluminescence spectra for InP/ZnS QDs synthesized with different amounts of $ZnSt_2$ and DDT during the shell growth process. (C) The photoluminescence spectra for InP/ZnS QDs synthesized with different zinc carboxylic and thiols during the shell growth process. The same mole amount of zinc undecylenate ($Zn(Unde)_2$), 1-octanethiol (OT), and 1-octadecanethiol (ODT) were used, compared to $ZnSt_2$ and DDT respectively.

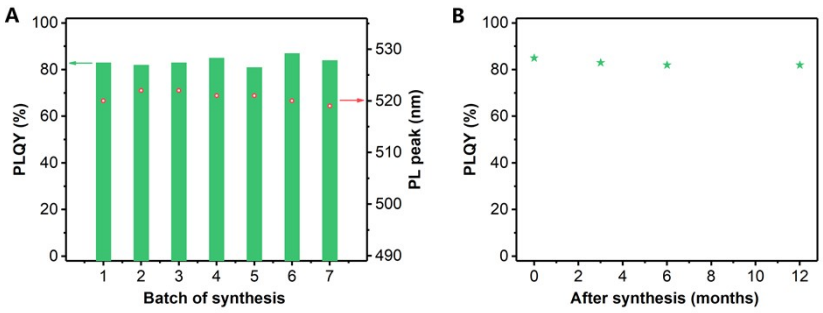

Figure S4. (A) PLQY and PL peak change for the repeated InP/ZnS QDs (InP/ZnS-DDT/300) synthesis. (B) PLQY change of InP/ZnS QDs (InP/ZnS-DDT/300) after storage in the fridge (2-6 °C).

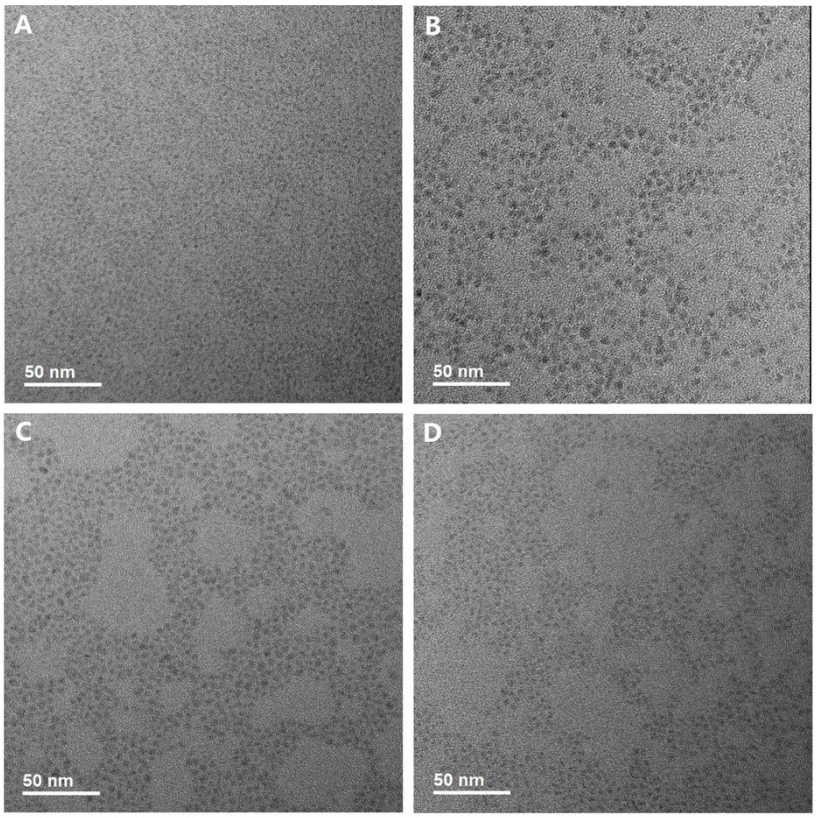

Figure S5. TEM images of (A) InP QDs, (B) InP/ZnS-DDT/300 QDs, (C) InP/ZnS-TOPS/300 QDs, (D) InP/ZnS-DDT/240 QDs.

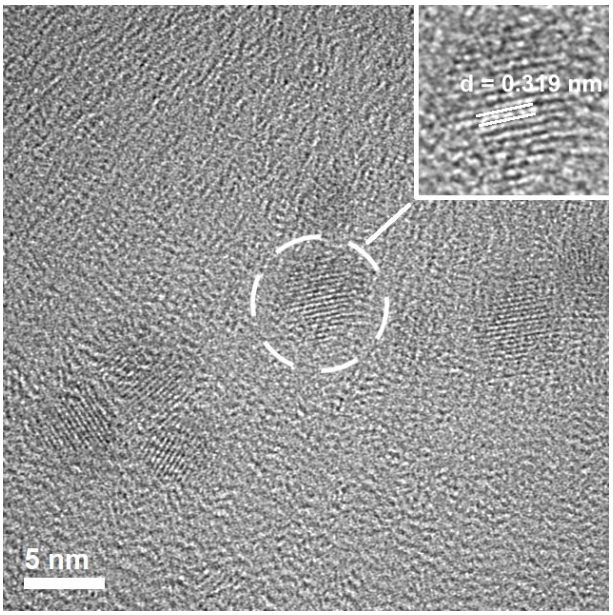

Figure S6. HRTEM image of InP/ZnS-DDT/300 QDs.

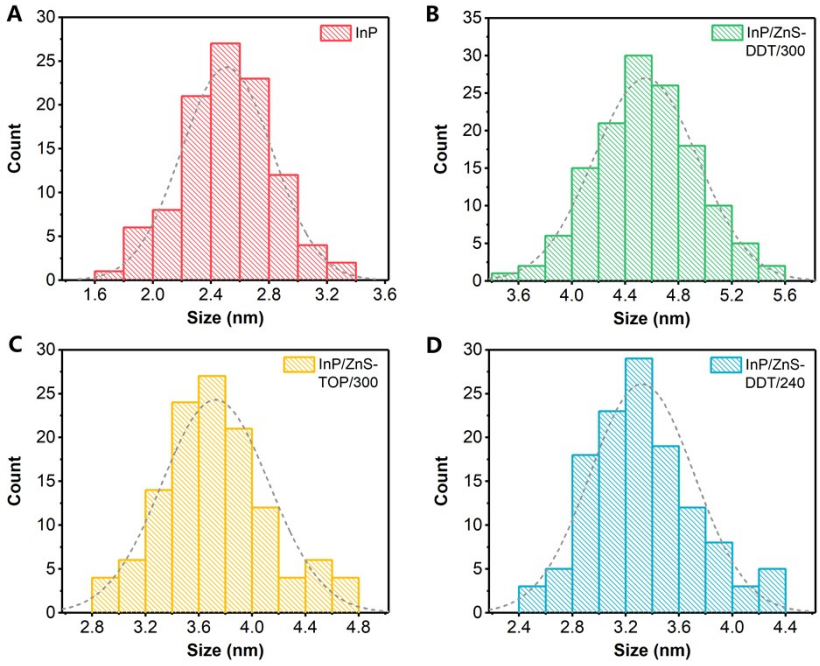

Figure S7. Size distribution analysis of (A) InP QDs, (B) InP/ZnS-DDT/300 QDs, (C) InP/ZnS-TOPS/300 QDs, (D) InP/ZnS-DDT/240 QDs.

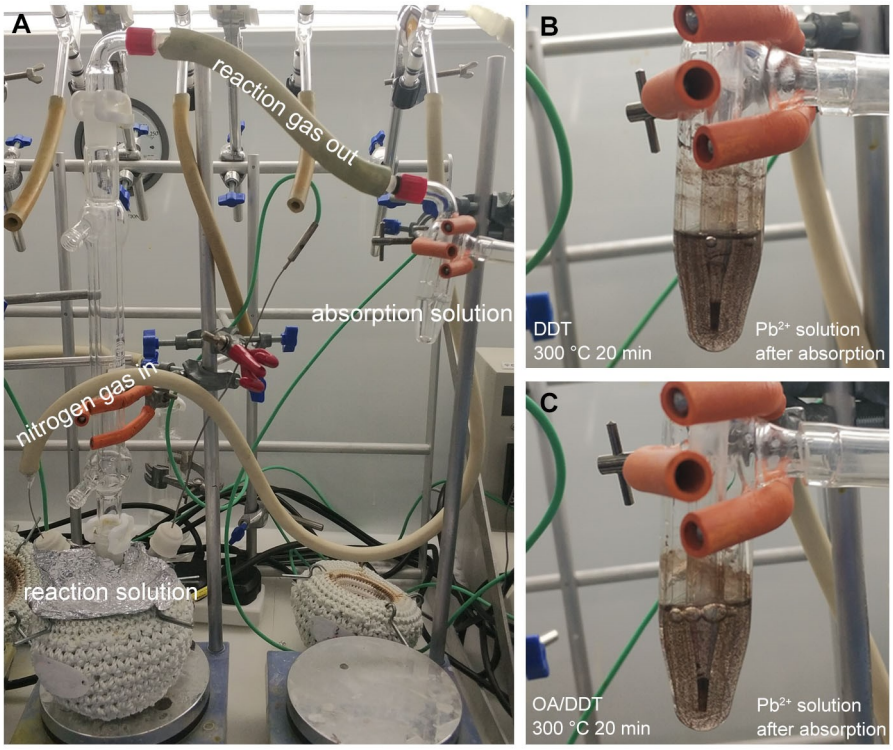

Figure S8. Detection of H_2S gas generated from the synthesis reactor. (A) Photograph of the reaction setup. Reaction condition: 5 mL ODE, 0.5 mL OLA or 0.5 mL OA, 0.8 mmol DDT or 0.4 mL 2 M TOPS at different heating temperatures. Test reagent (Pb^{2+} solution): 20 mg/mL $Pb(Ac)_2{\cdot}2H_2O$ aqueous solution. (B-C) Pb^{2+} solution after reaction under different conditions after 20 minutes: (B) DDT at 300 °C, and (C) OA/DDT at 300 °C.

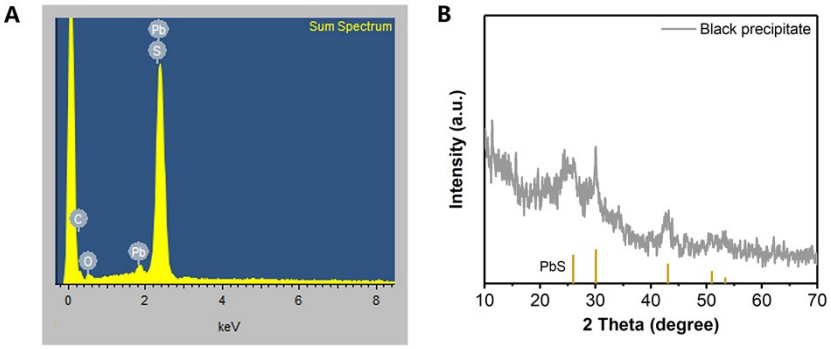

Figure S9. Characterization for the black precipitates during the H_2S absorption experiment: (A) SEM-EDS and (B) XRD. The PbS reference signal is taken from JCPDS No. 05-0592.

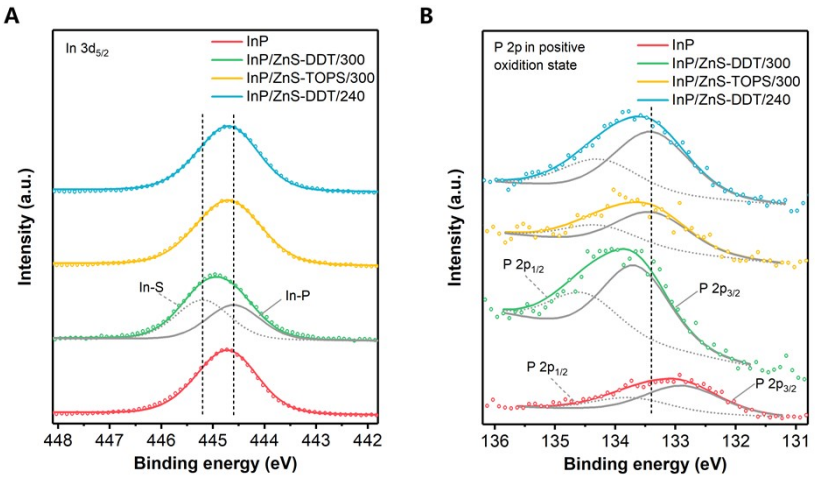

Figure S10. Fitting results of (A) In $3d_{5/2}$ and (B) P 2p in positive oxidization state of InP and InP/ZnS QDs in X-ray photoelectron spectra.

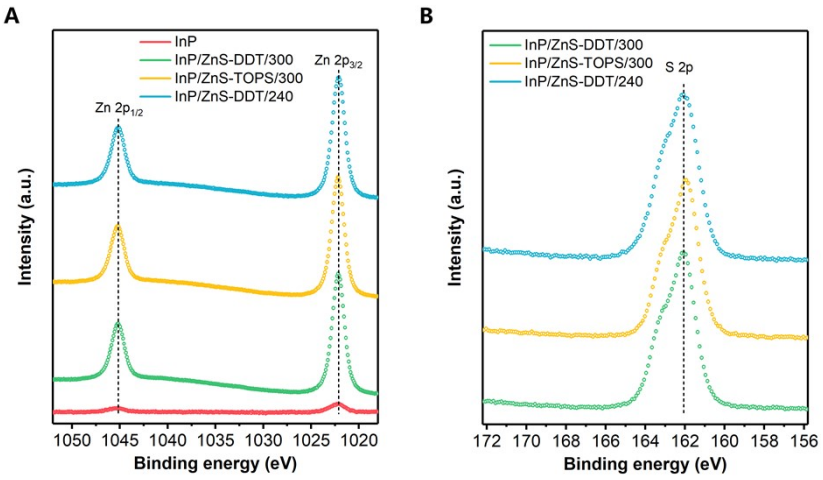

Figure S11. X-ray photoelectron spectroscopy profiles of (A) Zn 3d and (B) S 2p of InP and InP/ZnS QDs.

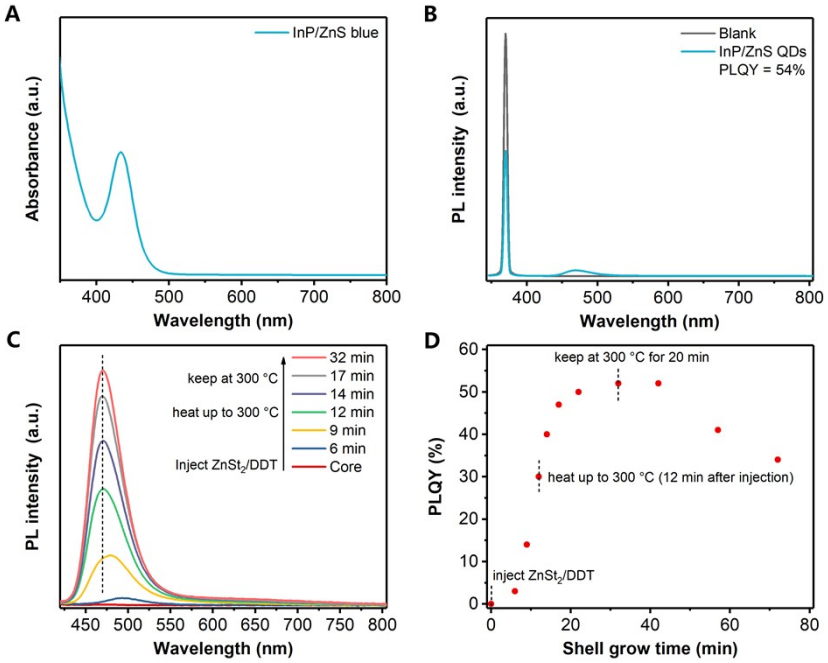

Figure S12. (A) Absorption spectrum of blue emission InP/ZnS QDs. (B) Absolute PLQY measurement of blue emission InP/ZnS QDs. (C) PL spectra and (D) the corresponding PLQY change of InP/ZnS QDs synthesized during different shell growth times. For the heating mantle used in our system, about 12 min are needed for the reaction solution to raise up to 300 °C.

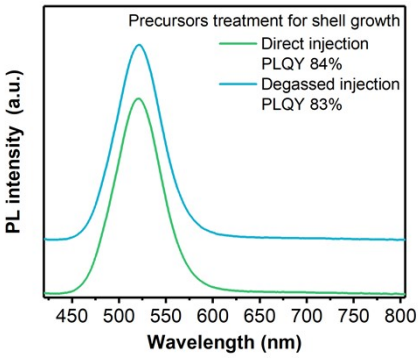

Figure S13. The PL comparison between InP/ZnS QDs synthesized with different treatment of precursors ($ZnSt_2$/ODE and DDT) during shell growth. In degassed injection, $ZnSt_2$ in ODE and DDT were put in two flasks separately. They were heated at 120 °C under the vacuum for 30 min and then turn to an N_2 atmosphere at 120 °C for another 30 min before injection.

Table S1. ICP-OES data for InP and InP/ZnS QDs synthesized under different conditions. QDs powders were treated with concentrated nitric acid for dissolution.

	In	P	Zn	S	p/In	Zn/In	S/In
	at%	at%	at%	at%	at%	at%	at%
InP	50.6	42.3	7.05	/	0.837	0.139	/
InP/ZnS-DDT/300	4.35	3.56	43.9	48.2	0.818	10.1	11.1
InP/ZnS-TOPS/300	9.67	8.62	40.6	41.1	0.891	4.19	4.25
InP/ZnS-DDT/240	12.3	10.5	33.7	43.5	0.859	2.75	3.55

*When calculating atom ratio (at%), only InP/ZnS crystal structure was considered (at% of In + P + Zn + S = 100%).

Table S2. SEM-EDS data for InP and InP/ZnS QDs synthesized under different conditions. Some results such as the S element in InP QDs and the I element in InP/ZnS QDs are not listed as the uncertainty at very low values.

	In at%	P at%	Zn at%	S at%	Cl at%	I at%
InP	39.7	32.4	7.69	/	14.6	5.26
InP/ZnS-DDT/300	3.96	2.99	44.8	44.3	3.65	/
InP/ZnS-TOPS/300	7.73	7.31	43.4	35.9	5.08	/
InP/ZnS-DDT/240	10.7	8.68	39.3	39.5	1.73	/

	P/In at%	Zn/In at%	S/In at%	Cl/In at%	I/In at%
InP	0.816	0.194	/	0.367	0.132
InP/ZnS-DDT/300	0.760	11.4	11.2	0.926	/
InP/ZnS-TOPS/300	0.948	5.63	4.65	0.657	/
InP/ZnS-DDT/240	0.822	3.75	3.73	0.165	/

Table S3. Kinetic analyses of emission decay for InP and InP/ZnS QDs.

	τ_1(ns)	B_1	τ_2(ns)	B_2	τ_3(ns)	B_3	τ_{avg}(ns)
InP	3.03	2164	16.4	343	101	55.6	37.9
InP/ZnS-DDT/300	/	/	54.3	2474	140	342	76.6
InP/ZnS-TOPS/300	/	/	49.7	2119	121	652	80.2
InP/ZnS-DDT/240	/	/	35.7	1795	106	732	74.1

The PL emission decay traces for InP and InP/ZnS QDs were well fitted with double or triple-exponential function Y(t) based on nonlinear least-squares, using the following equation (1):

$$Y(t) = B_1 exp(-t/\tau_1) + B_2 exp(-t/\tau_2) + B_3 exp(-t/\tau_3) \quad (1)$$

Where B1, B2, B3 are fractional contributions of time-resolved emission decay lifetimes τ1, τ2, τ3 and the average lifetime <τ> can be concluded from the equation (2):[1, 2]

$$\langle\tau\rangle = (B_1\tau_1^2 + B_2\tau_2^2 + B_3\tau_3^2)/(B_1\tau_1 + B_2\tau_2 + B_3\tau_3) \quad (2)$$

Table S4. SEM-EDS data for InP/ZnS QDs synthesized with $ZnSt_2$ and S at 300 °C.

	In at%	P at%	Zn at%	S at%	Cl at%	I at%
InP/ZnS-S/300	1.65	1.89	46.2	45.2	4.29	/

	P/In at%	Zn/In at%	S/In at%	Cl/In at%	I/In at%
InP/ZnS-S/300	1.14	27.9	27.3	2.59	/

Table S5. SEM-EDS data for InP/ZnS-TOPS/300 and InP/ZnS-DDT/240 QDs before and after additional purification.

	P/In at%	Zn/In at%	S/In at%	Cl/In at%	I/In at%
InP/ZnS-TOPS/300	3.28	3.24	1.25	0.472	/
InP/ZnS-TOPS/300 additional purification	0.948	5.63	4.65	0.657	/
InP/ZnS- DDT/240	1.52	4.27	4.39	0.176	/
InP/ZnS-DDT/240 additional purification	0.822	3.75	3.73	0.165	/

Table S6. PL information for InP/ZnS-TOPS/300 and InP/ZnS-DDT/240 QDs before and after additional purification.

	PL peak	FWHM	PLQY
InP/ZnS-TOPS/300	544 nm	66 nm	49%
InP/ZnS-TOPS/300 additional purification	542 nm	66 nm	43%
InP/ZnS-DDT/240	538 nm	65 nm	39%
InP/ZnS-DDT/240 additional purification	537 nm	65 nm	42%

Supplemental Methods

Materials

$InCl_3$ (99.99%), $ZnCl_2$ (98%), sulfur (S, 99%), selenium (Se, 99.5%), 1-octadecene (ODE, 90%), trioctylphosphine (TOP, 90%), oleic acid (OA, 90%) were obtained from Alfa Aesar; ZnI_2 (98%), tris(diethylamino)phosphine (97%), zinc stearate ($ZnSt_2$, 10-12% Zn basis), zinc undecylenate (98%) 1-dodecanethiol (DDT, 98%), 1-octanethiol (98.5%), 1-octadecanethiol (98%) were obtained from Sigma-Aldrich; oleylamine (OLA, C18 content 80%-90%) was obtained from Acros Organics; hexane (HEX, 95%), ethanol (EtOH, 99.8%), isopropanol (IPA, 99.8%) and acetone (99.8%) were obtained from Fisher Scientific. To avoid possible oxidation or moisture absorption, the chemicals which are not stable in the air were well stored in the glovebox.

Characterization

UV-vis absorption spectra were recorded on Agilent Cary 7000 UMS spectrophotometer. Photoluminescence and photoluminescence quantum yield were measured by UV-NIR absolute PLQY spectrometer (HAMAMATSU, Quantaurus-QY plus; excitation wavelength 370 nm). PL intensity was normalized by either the peak intensity or the absorbed photonics. Transmission electron microscopy (TEM) was performed on a Tecnai F20 microscope (operated at an accelerating voltage of 200 kV). X-ray diffraction patterns were recorded on a Bruker D8 Advance powder X-ray diffractometer, with Cu-K_α radiation at λ = 1.54 Å. Elemental analysis of ICP-OES was determined on a Thermo Scientific iCAP 7400 ICP-OES DUO spectrometer. SEM-EDS investigations were performed on a LEO GEMINI 1530VP FEG-SEM instrument (operated at an accelerating voltage of 15 kV). QDs powders were spread on Cu conducting resins for measurement and each measurement was repeated by 3 scans or more on different areas. XPS data collection was performed at the EPSRC National Facility for XPS (HarwellXPS). The binding energy was calibrated using the C 1s peak at 284.8 eV. When used for comparison, the binding energy in literature was tuned based on the same C 1s calibration value. Transient photoluminescence spectra (time-correlated single photon counting) was recorded on Edinburgh Instruments FLS900 photoluminescence spectrometer (excitation wavelength 406 nm).

Transient absorption spectroscopy is used to measure the short lifetime (< 2 ns). The setup is described as follows. The output of a Ti:sapphire amplifier system (Spectra Physics Solstice Ace) operating at 1 kHz and generating ~100 fs pulses (fundamental, 800 nm) was split into pump pulses and probe pulses. The 400 nm pump pulses were created by sending the 800 nm fundamental beam of the Solstice Ace through a second harmonic generating beta barium borate (BBO) crystal (Eksma Optics). The pump was blocked by a chopper wheel rotating at 500 Hz. The broadband probe (330-700 nm) was generated by focusing the 800 nm fundamental beam onto a CaF_2 crystal (Eksma Optics, 5 mm) connected to a digital motion controller (Mercury C-863 DC Motor Controller). The pump-probe delay (100 fs to 2 ns) was controlled by a mechanical delay stage (Thorlabs DDS300-E/M). The transmitted pulses were collected with a monochrome line scan camera (JAI SW-4000M-PMCL, spectrograph: Andor Shamrock SR-163). The spectra were taken with liquid samples inside a 1 mm thick cuvette. Concentration of samples was adjusted to an absorbance of 1 OD at 400 nm. The energy fluence obtained on the sample was ~150 μJ/cm^2.

The detection of H_2S gas was performed in two ways. In the first method, the reaction gas flowed through a pipe and went into a Pb^{2+} solution (Figure S8A). Reaction conditions: 5 mL ODE, 0.5 mL OLA or 0.5 mL OA, 0.19 mL DDT or 0.4 mL 2 M TOPS under N_2 atmosphere and were heated at different temperatures. The detecting Pb^{2+} solution is made of 20 mg/mL $Pb(Ac)_2{\cdot}2H_2O$ aqueous solution. In the second method, gas chromatography with flame photometric detector (GC-FPD, Huifen GCS-90) was used to monitor the possible gas generation. The reaction gas was extracted from the flask and injected into the GC-FPD. Reaction conditions: 5 mL ODE, 0.125 mL OLA, 0.048 mL DDT or 0.1 mL 2 M TOPS under Ar atmosphere and were heated at different temperatures. Note that considering the safety issue and the upper detected limitation, concentration of the reactants used for H_2S detection was reduced compared to those in QDs synthesis.

QDs synthesis

Synthesis of InP QDs and InP/ZnS QDs for green emission.

InP core QDs were synthesized based upon a modified literature protocol.[3] 111 mg (0.5 mmol) of $InCl_3$, 204 mg (1.5 mmol) of $ZnCl_2$ and 160 mg (0.5 mmol) of ZnI_2 were mixed in 5.0 mL (15 mmol) of oleylamine in 50 mL 3-neck round flask. The reaction mixture was then evacuated by Schlenk techniques and kept under vacuum at 120 °C for at least 30 min. Afterwards, the system was heated to 170 °C under an inert atmosphere. 0.5 mL (1.8 mmol) of tris(diethylamino)phosphine (P: In = 3.6: 1) was then quickly injected into the mixture. InP QDs synthesis proceeded for 20 min.

For the typical synthesis of InP/ZnS QDs (named InP/ZnS-DDT/300 QDs), after the InP QDs formation at 170 °C by reaction of 20 min, 1.26 g (2 mmol) $ZnSt_2$ dispersed in 5 mL ODE with 1.90 mL (8 mmol) DDT were injected into the above InP QDs solution. The reaction solution was then heated to 300 °C and kept at 300 °C for 1 hour for the shell growth. Finally, the system was cooled down to room temperature naturally. During ZnS shell growth, a complete degassing for precursors ($ZnSt_2$ in ODE and DDT) was not necessary (Figure S13).

After cooling down, 10 mL of hexane was introduced to the crude QD solution. The mixture was centrifuged at 8000 rpm for 5 min, and the supernatant QDs solution was collected. Then 40 mL of ethanol was added for the precipitation of QDs. After centrifugation at the same condition, the collected QDs precipitates were further dissolved in 10 mL of hexane. Then, addition of 20 mL of ethanol is used for the second-time precipitation and purification of QDs with similar operations. Finally, the purified QDs were dissolved in hexane. After passing through a 0.45 μm filter, the QDs solution was kept in the fridge (2-6 °C) for long time storage.

Synthesis of InP/ZnS QDs with other shell growth conditions.

To investigate the effect of various ZnS shell growth methods, different experimental conditions were applied. Apart from the variate parameter, other synthetic processes were kept the same as above InP/ZnS-DDT/300 QDs. For example, when using S dissolve in TOP (TOPS) as the S source for the shell growth (named InP/ZnS-TOPS/300 QDs), 256 mg (8 mmol) sulfur was dissolved in 4 mL of TOP by heating under an inert atmosphere. We also changed the temperature for shell growth with DDT, named InP/ZnS-TOPS/240 QDs, which was kept at 240 °C for 1 hour for shell growth after formation of InP QDs.

Note that the purification process may slightly differ from the standard process above. When preparing QDs powders, we find that additional purification is needed to remove unreacted precursors and by-products. Otherwise, some analyses may be inaccurate, especially for the InP/ZnS-TOPS/300 and InP/ZnS-DDT/240 QDs (See details in Supplemental Methods; Tables S5 and S6).

Synthesis of InP/ZnS QDs for other emission wavelengths.

To synthesize InP/ZnS QDs for other emission wavelengths, different amounts of Zn precursor ($ZnCl_2$ and ZnI_2) were used at the beginning of InP core formation. For InP/ZnS QDs with blue emission, 640 mg (2 mmol) ZnI_2 was used as the Zn precursor during InP core synthesis. The time for ZnS shell growth at 300 °C was 20 min. For InP/ZnS QDs with orange emission, 272 mg (2 mmol) $ZnCl_2$ was used as the Zn precursor during InP core synthesis. The time for ZnS shell growth at 300 °C was 60 min. For InP/ZnS QDs with red emission, 272 mg (2 mmol) $ZnCl_2$ was used as the Zn precursor during InP core synthesis, and tris(diethylamino)phosphine was injected twice for larger InP core size. Briefly, 0.25 mL tris(diethylamino)phosphine was quickly injected. After 10 min, another 0.25 mL tris(diethylamino)phosphine was dropwise within 10 min. The time for ZnS shell growth at 300 °C was 30 min.

Additional purification for InP/ZnS QDs.

During characterization, we found that InP/ZnS QDs with general purification might contain some impurities. In particular, the ratio of P to In is unexpectedly high in InP/ZnS-TOPS/300 and InP/ZnS-DDT/240 QDs (Table S5). It is noticed that some literature for InP synthesis with aminophosphine also reported significantly high ratios of P to In.[4, 5] Therefore, the additional selective purification of these two kinds of QDs with different volume of hexane and ethanol were applied. Briefly, for InP/ZnS-DDT/240 QDs, we find that a small volume of ethanol help removes the impurities. After diluting the QDs with hexane, ethanol (ethanol/hexane: v/v = 1:1) was added for precipitation. The dissolution and precipitation process were further repeated two or three times (Table S5). For InP/ZnS-TOPS/300 QDs, we diluted the QDs with hexane and then added ethanol (ethanol/hexane: v/v = 0.6:1). Then white precipitates appeared, and the supernatant was still coloured as QDs. After centrifugation, the supernatant QDs solution was further precipitated by introducing more ethanol (total ethanol/hexane: v/v = 1.5:1) to precipitate the QDs (Table S5).

The higher ratio of P is unlikely coming from InP as the InP core has an In-rich surface. For InP/ZnS-DDT/240 QDs, we assume the excess of P is caused by P-related residuals adsorbed on the surface of QDs.[6, 7] For InP/ZnS-TOPS/300 QDs, the ratio of Zn to S is also unexpected higher besides of P to In (Table S5). Therefore, we speculate Zn-P organometallic complex or metastable structure was formed in the solution along with ZnS shell growth, where the P source is likely coming from the by-product $P(NHR)_4Cl$ and/or TOP from TOPS. It is reported zinc phosphide nanocrystals can be formed from Zn^{2+} and TOP at high temperature after a long reaction time,[8] showing the possibility of zinc phosphide impurities in our synthesis.

Control experiments show that the PL properties are little affected by the impurities for InP/ZnS-TOPS/300 and InP/ZnS-DDT/240 QDs (Table S6), probably due to that the impurities do not absorb or emit light at the measured wavelength. However, for some other measurements like element analysis,

this additional purification is essential to get an accurate result.

Supplemental References

1. S. N. Sharma, Z. S. Pillai and P. V. Kamat, *J. Phys. Chem. B*, 2003, **107**, 10088-10093.
2. C. Higgins, M. Lunz, A. L. Bradley, V. A. Gerard, S. Byrne, Y. K. Gun'ko, V. Lesnyak and N. Gaponik, *Opt. Express* 2010, **18**, 24486-24494.
3. S. Yu, X.-B. Fan, X. Wang, J. Li, Q. Zhang, A. Xia, S. Wei, L.-Z. Wu, Y. Zhou and G. R. Patzke, *Nat. Commun.*, 2018, **9**, 4009.
4. Y.-C. Pu, H.-C. Fan, J.-C. Chang, Y.-H. Chen and S.-W. Tseng, *J. Phys. Chem. Lett.*, 2021, **12**, 7194-7200.
5. F. Huang, C. Bi, R. Guo, C. Zheng, J. Ning and J. Tian, *J. Phys. Chem. Lett.*, 2019, **10**, 6720-6726.
6. M. D. Tessier, K. De Nolf, D. Dupont, D. Sinnaeve, J. De Roo and Z. Hens, *J. Am. Chem. Soc.*, 2016, **138**, 5923-5929.
7. J. L. Stein, W. M. Holden, A. Venkatesh, M. E. Mundy, A. J. Rossini, G. T. Seidler and B. M. Cossairt, *Chem. Mater.*, 2018, **30**, 6377-6388.
8. M. H. Mobarok, E. J. Luber, G. M. Bernard, L. Peng, R. E. Wasylishen and J. M. Buriak, *Chem. Mater.*, 2014, **26**, 1925-1935.